01 Jan 2014

Development of a Tribometer to Characterize Lubrication Layer Properties of Self-Consolidating Concrete

Dimitri Feys
Missouri University of Science and Technology, feysd@mst.edu

Kamal Khayat
Missouri University of Science and Technology, khayatk@mst.edu

Aurelien Perez-Schell

Rami Khatib

Recommended Citation

D. Feys et al., "Development of a Tribometer to Characterize Lubrication Layer Properties of Self-Consolidating Concrete," *Cement and Concrete Composites*, vol. 54, pp. 40 - 52, Elsevier, Jan 2014.
The definitive version is available at https://doi.org/10.1016/j.cemconcomp.2014.05.008

Cement & Concrete Composites 54 (2014) 40–52

Contents lists available at ScienceDirect

Cement & Concrete Composites

journal homepage: www.elsevier.com/locate/cemconcomp

Development of a tribometer to characterize lubrication layer properties of self-consolidating concrete

Dimitri Feys [a,*], Kamal H. Khayat [a,b], Aurelien Perez-Schell [b], Rami Khatib [b]

[a] Department of Civil, Architectural and Environmental Engineering, Missouri University of Science and Technology, Rolla, MO, United States
[b] Department of Civil Engineering, Université de Sherbrooke, QC, Canada

ARTICLE INFO

Article history:
Received 14 November 2013
Received in revised form 15 April 2014
Accepted 21 May 2014
Available online 6 June 2014

Keywords:
Lubrication layer
Highly-workable concrete
Rheology
Tribometer
Self-consolidating concrete
Viscous constant

ABSTRACT

The last decade, significant advances have been made in investigating, understanding and predicting the flow characteristics during pumping of concrete. Kaplan developed theoretical equations based on the rheological and tribological properties of concrete to predict pumping pressures. Several tribometers were developed to characterize the flow properties of concrete along a smooth wall, but none of them allows the use of highly-workable concretes. The main reason is that for the calculation of the yield stress and viscous constant of the lubrication layer, the concrete is not allowed to be sheared.

In this paper, a new design for the concrete tribometer is presented, along with a calculation procedure to eliminate the contribution of concrete shearing from the rotational velocity. In this way, the viscous constant can be calculated in the same way as for the previously developed tribometers. The analysis of the data reveals that the total flow resistance in the tribometer (I_{trib}) is well related to the plastic viscosity for SCC and to the yield stress for the other concretes, which is in line with practical results on the influence of rheology on pumping pressure. The viscous constant of the lubrication layer appears related to the plastic viscosity of SCC, but the paper shows that many mix design parameters influence this relationship.

1. Introduction

In the past, many attempts have been made to estimate the pressure during pumping of concrete [1–10]. Based on practical experience, several guidelines were developed to predict pressure as a function of the discharge rate, length of the circuit, concrete consistency, etc. [11–13]. Several practical guidelines for quantifying the effect of bends and reducers, for minimum paste volume and minimum sand-to-total aggregate ratio were proposed to reduce problems occurring during pumping of concrete [11–14].

Kaplan [6,15] developed a fundamental model describing the pressure loss during pumping in straight pipes, based on the rheological properties of the concrete and the properties of the lubrication layer (also called boundary layer). During pumping of concrete, aggregates tend to move to the center of the pipe, while a more fluid layer, rich with cement paste, is formed near the wall; this layer is called the lubrication layer. In the work of Kaplan [6], the rheological properties of the concrete are described by the Bingham model, identifying a yield stress (Pa) and a plastic viscosity (Pa s) [16]. These properties can be measured with different commercially available rheometers. The properties of the lubrication layer need to be measured with a so-called tribometer, which is a device, similar to a rheometer, which allows the formation of the lubrication layer near one of the rotating parts. Indeed, in contrast to a concrete rheometer, where horizontal segregation is prevented (or at least minimized) by the presence of protruding ribs or a vane, a tribometer contains a smooth wall allowing the creation of the more fluid cement-paste layer.

During pumping, conventional vibrated concrete (CVC) is known to move as a plug in pipes, surrounded by the lubrication layer [2–6]. This layer takes all the shearing and allows the concrete to be pumped. For highly-workable concrete (HWC – slump flow in the range of 400–600 mm) and self-consolidating concrete (SCC – slump flow larger than 600 mm), the relatively low yield stress [17,18] of the material causes also a part of the concrete to be sheared during pumping, in addition to the shearing of the lubrication layer. This is taken into account in the model of Kaplan [6], which contains an equation for both flow conditions. On the other hand, the characterization of the lubrication layer in a tribometer requires, up to now, that the concrete in the tribometer is not sheared, and that the entire velocity difference occurs in the lubrication layer. As a result, the lubrication layer properties of highly-workable concrete are more difficult to be quantified.

* Corresponding author. Tel.: +1 573 341 7193; fax: +1 573 341 4729.
E-mail address: feysd@mst.edu (D. Feys).

http://dx.doi.org/10.1016/j.cemconcomp.2014.05.008
0958-9465/

List of symbols

H	height (m)
I_{trib}	total flow resistance in tribometer (Nms) = slope T–N line
N	rotational velocity (rps)
R	radius of cylinder (m)
T	torque (N m)
V	linear velocity (m/s) = $2\pi NR$
$\dot{\gamma}$	shear rate (s^{-1})
η	viscous constant (Pa s/m)
μ_p	plastic viscosity (Pa s)
τ	shear stress (Pa)
τ_0	yield stress (Pa)

Indices

cone	cone of the developed tribometer
i	inner, mostly reflecting the inner cylinder
LL	lubrication layer
o	outer, mostly reflecting the outer cylinder
p	plug, boundary between sheared and unsheared zone

This paper describes the development of a new tribometer for HWC. It discusses how the lubrication layer properties are obtained and provides a short description of the currently available tribometers. These tribometers are judged not suitable for HWC, mainly because the low yield stress of HWC and SCC causes the bulk concrete to be sheared, which is in contrast to the basic assumption for tribology. As a consequence, complex 3-D flows, or large variations in shear rates inside the tribometer make these apparatuses less reliable for HWC and SCC. The newly developed tribometer and data treatment procedure accounts for the shearing in the bulk concrete and delivers an approximate correction for the secondary flow effects. Finally, the results of a series of tests are discussed by comparing the flow behavior in the tribometer (total flow resistance and the viscous constant of the lubrication layer) to the rheological properties and mix designs of the tested concretes.

2. Quantification of lubrication layer properties

The properties of the lubrication layer are quantified in a similar way as the rheological properties of cementitious materials. The configuration of a tribometer is based on the principle of coaxial cylinders, where one cylinder rotates relatively to the other. At various rotational velocities, the resulting torque is measured. For rheology, the data points, expressed as torque as a function of rotational velocity, can be transformed into shear stress–shear rate data, using the Reiner–Riwlin equation [19,20]. If in a rheometer, only a part of the material is sheared due to the presence of a plug, the shear stress–shear rate data must be calculated iteratively, as the plug radius would depend on the yield stress of the material.

In contrast to rheology, the determination of the properties of the lubrication layer does not involve a homogeneous material. Theoretically, the material in the tribometer could be divided into two zones: The cement-paste (or micromortar) constituting the lubrication layer, and the bulk concrete. For CVC (and any other concrete type with a rather high yield stress), all shearing is concentrated in the lubrication layer [6,8]. The torque can easily be transformed into a shear stress (in Pa) at the inner cylinder, as this is the place where the lubrication layer forms (Eq. (1)).

$$\tau_i = \frac{T}{2\pi R_i^2 h} \tag{1}$$

The yield stress of the lubrication layer can be obtained by the extrapolation of the obtained τ–V curve to zero velocity. The calculation of the viscosity (in Pa s) is not evident, as it would require the determination of the thickness of the lubrication layer to calculate the shear rate. Until now, no precise method has been described to measure the thickness of this layer inside a tribometer. Consequently, a new parameter has been defined by Kaplan [6]: The viscous constant (in Pa s/m), which is simply the slope of the line in a shear stress–linear velocity diagram. As a result, the properties of the lubrication layer are described by Eq. (2) [6,8]:

$$\tau_{LL} = \tau_{0,LL} + \eta_{LL} V \tag{2}$$

The linear velocity can be easily determined as the product of the inner cylinder radius and the angular velocity, or as $2\pi R_i N$, with N being the rotational velocity (in rps).

It should be noted that for the derivation of Eq. (2), a constant shear rate in the lubrication layer is assumed [6,8]. This is justified by the small thickness of the lubrication layer, reflecting the case of a narrow gap coaxial cylinders rheometer [21].

3. Description of available tribometers

In this section, the three different tribometers that can be used with the pressure prediction model of Kaplan are briefly described. The restrictions on using these tribometers to determine the tribological characteristics of HWC are commented. An overview of the different tribometers and their restrictions is given in Fig. 1.

Kaplan [6] modified the BTRheom [22] to obtain a concentric cylinders tribometer (Fig. 1: top). The main problem with the modified BTRheom is the sealing between the stationary bottom plate and the rotating inner cylinder. This sealing is provided by a rubber strap, which causes an additional torque during measurement. An idle measurement before loading the concrete in the tribometer provides a correction factor, but with intense application, cement paste and sand particles get attached to the seal, thus progressively increasing its resistance during flow. Although the rubber seal is a disadvantage, this kind of tribometer has been successfully used for CVC.

In order to overcome the problem with the rubber seal in the Kaplan tribometer, Chapdelaine [8] developed a new type of tribometer, based on the Tattersall Mk-III rheometer [16] (Fig. 1: middle). The rotating device is an open cylinder, while the concrete bucket is equipped with ribs at the outer wall and a small vane is installed in the center. The main advantage of this tribometer, is that it does not require the installation of a rubber seal.

In his research, Ngo [23] developed a portable variation of the modified BTRheom. It consists of a closed cylinder which is rotated in a bucket of concrete, maintaining a clear spacing between the bottom of cylinder and the bottom of the bucket (Fig. 1: bottom). By inducing the spacing, the necessity of a seal is avoided. To eliminate the influence of the bottom part of the inner cylinder, the determination of the lubrication layer properties is done in two steps. In the first step, the bucket is filled with concrete in a way that the bottom of the inner cylinder touches the upper concrete surface, and a first sweep of the velocity curve is performed. In the second step, the concrete bucket is entirely filled, and the same velocities are applied to the inner cylinder. The properties of the lubrication layer of CVC can thus easily be determined when subtracting step 1 from step 2.

The main difficulties that arise if these tribometers would be used for HWC, including SCC, is the shearing of the bulk concrete, as HWC and SCC have relatively low yield stresses that are likely to

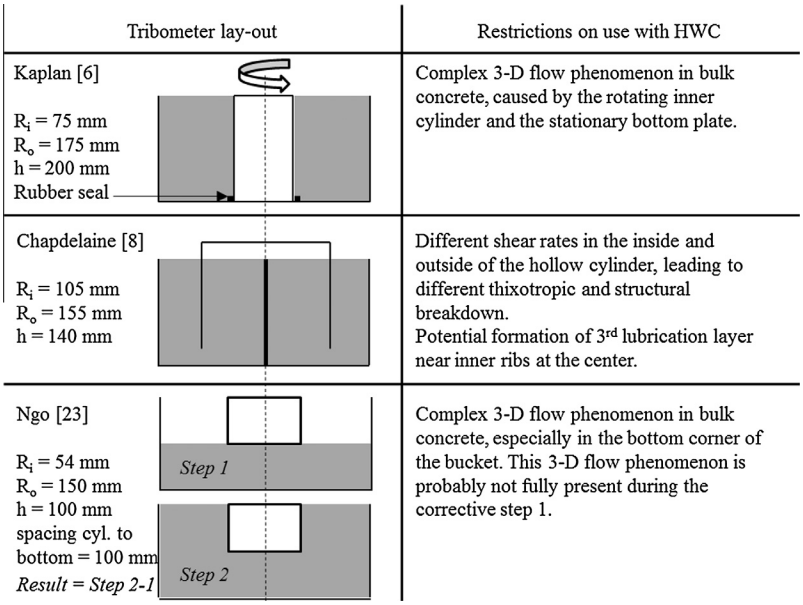

Fig. 1. Concept of tribometers developed by Kaplan, Chapdelaine and Ngo and short statement why they are not applicable on HWC.

be exceeded. The shearing would cause complex 3-dimensional velocity patterns in the Kaplan and Ngo tribometers that cannot be easily taken into account. For the Chapdelaine tribometer, the shear rate on the inside or the outside of the rotating hollow cylinder will be different, leading to differences in thixotropic or structural breakdown [24]. Furthermore, due to the very high shear rate near the inner ribs in this tribometer, the formation of a third lubrication layer cannot be excluded.

A different way of characterizing the flow resistance in pipes is to observe the flow of concrete induced by gravity through a pipe. The relationship between the flow rate and the quasi-hydrostatic head of concrete gives an indication of the flow resistance. With this method, Jacobsen et al. [25] showed the influence of concrete composition and the influence of the pipe material on the flow resistance. However, the flow through pipes induced by gravity is slow compared to real pumping and it can be questioned if the flow conditions obtained by gravitational flow are fully applicable to full-scale pumping [26,27]. Note also that in this case, the lubrication layer properties are not applicable to the model proposed by Kaplan, and that extrapolation of the results to realistic flow rates may lead to erroneous results.

4. Development of new concrete tribometer

4.1. Description

The new tribometer is based on the modified Tattersall Mk-III [16], similar to the one used by Chapdelaine [8]. The planetary motion of the impeller is removed, and the H-impeller is replaced by a steel cylinder with a radius of 62.5 mm and a height of 200 mm (Fig. 2). The bottom of the cylinder has a conical shape, with an additional height of 50 mm. As a result, the angle of the cone relative to the bottom of the reservoir is 38.7°. The reservoir of the Mk-III is replaced by a smaller version, to limit the amount of concrete used. The radius of the reservoir measures 118.5 mm, while the height is 260 mm. The total amount of concrete needed to run the test is 8.8 l.

As the reservoir is first filled with concrete, the conical shape at the bottom of the inner cylinder assures a rather easy insertion of the inner cylinder in the concrete when lifting the bottom plate. The clear spacing between the cone tip and the bottom plate is around 10 mm. It can be argued that this spacing is rather small and certainly induces some secondary flow effect. On the other hand, the height of the inner cylinder is 200 mm, causing the effect of the bottom to be small compared to the measured values of the torque.

As the tribometer is installed on a portable version of the Tattersall Mk-III rheometer, it can be used on a job site. A computer attached to the tribometer is used for data processing and saving.

4.2. Testing procedure

The testing procedure applied in the tribometer is similar to a testing procedure applied for a standard concrete rheometer. The rotational velocity is decreased in 10 steps from around 0.9 to 0.01 rps, holding the rotational velocity constant at each step during 5 s. At each rotational velocity, the resulting torque is registered. The testing procedure is preceded by a 30 s pre-shearing period at 0.9 rps (Fig. 3). This pre-shearing period allows for the lubrication layer to be created and would eliminate the effect of thixotropy on the measured results.

The maximum rotational velocity is chosen as high as possible (it is the upper limit of the engine of the device), in an attempt to attain typical flow rates during pumping. However, the velocity in the tribometer is still lower than in real case pumping. On the other hand, in contrast to concrete rheometry, the maximum rotational velocity must not be reduced to avoid horizontal migration of the aggregates, as a lubrication layer needs to be created. Secondly, the test is performed in a short time-span to minimize the influence of loss of workability and thixotropic rebuild on the obtained results. Once equilibrium is achieved during the pre-shearing period, the time steps on the decreasing velocity curve can be kept short.

4.3. Evaluation of secondary flow effect caused by the cone

As mentioned in Section 3, secondary flows occur between the stationary bottom of the concrete bucket and the rotating inner cylinder, especially when employing HWC. With the development of the new tribometer, a special procedure was employed to isolate the secondary flow effects. The procedure consisted of testing nine concrete mixtures with different rheological properties at six

Fig. 2. Portable tribometer developed at the Université de Sherbrooke for testing the tribological properties of highly-workable concretes, including self-consolidating concrete.

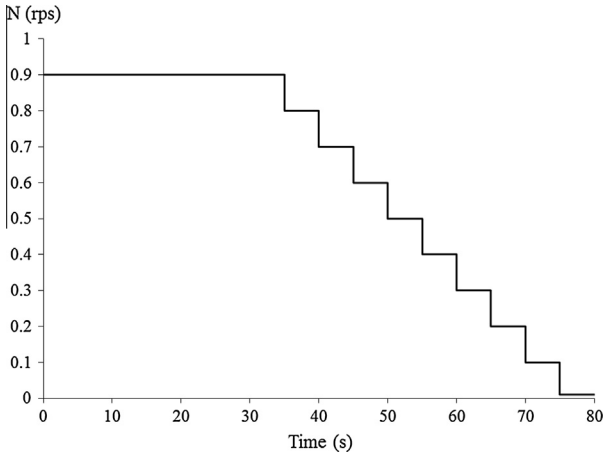

Fig. 3. Schematic representation of the imposed rotational velocity during a tribometer test.

different filling heights in the tribometer. The composition and rheological properties of these concretes can be found in Table 1. Although this approach is theoretically the best procedure [21], it did not deliver consistent results. In theory, with this procedure, the torque at each rotational velocity should be a linear function of the filling height (of the cylindrical part). The value at the origin ($h = 0$) corresponds to the influence of the bottom effect, as the reference height (0) is taken at the bottom of the cylindrical part of the inner cylinder. A filling height equal to zero means thus that the conical part is completely submerged in the concrete, while the cylindrical part is completely free.

The experiments, however, did deliver an approximate linear function between total torque and filling height, but it was not perfect. The extrapolation of the best fitting line to zero filling height induces thus an error which is related to the error in measurements. This error can be due to several reasons: of which the precision of the measuring equipment is one of them. Secondly, as the filling height increased, the rotational velocity at each step decreased slightly. This is attributed to the electrical power sent to the engine of the tribometer, as the more resistance the engine has, the slower it will rotate. Thirdly, errors could be attributed to the testing procedure. As for each test, a certain volume of concrete was added to increase the filling height, the previous concrete was not removed to avoid the time-consuming job of emptying and cleaning. Emptying and cleaning would cause a significant time delay between the tests at different heights, inducing the error caused by loss of workability. Adding a new layer of concrete on the older layers to increase the height can induce differences in properties of concrete due to errors in sampling and a difference in shear history. For the lower layers, the lubrication layer has been formed during previous tests, while for the new layer, the lubrication layer still has to be created. Although macroscopically, no significant decrease in values at each velocity step was observed after the 30 s pre-shearing period, it could be that some slight variation (decrease in properties of lubrication layer or increase in thickness)

Table 1
Mix designs (per m^3) of concretes used for the investigation of the influence of the cone. GU = GU Cement, Si.F. = silica fume, F.A. F = class F fly ash.

	GU (kg)	Si.F. (kg)	F.A. F (kg)	Water (kg)	Sand (kg)	Aggr. (kg)	SP (l)	w/cm (–)	τ_0 (Pa)	μ_p (Pa s)
SCC 1-1	402	48	150	186	816	719	2.5	0.31	40	24
SCC 1-2	402	48	150	186	816	719	2.5	0.31	67	28
SCC 2	581	37	–	173	865	762	4.9	0.28	0	74
SCC 3-1	581	37	–	155	890	785	6.3	0.25	0	129
SCC 3-2	581	37	–	155	890	785	6.3	0.25	0	141
SCC 4-1	402	48	150	168	842	741	3.7	0.28	14	41
SCC 4-2	402	48	150	168	842	741	3.7	0.28	20	43
SCC 5	397	35	144	161	867	764	3.4	0.28	24	63
HWC 6	397	35	143	161	803	830	2.8	0.28	212	99

still occurs when the top layer undergoes for the first time the decreasing velocity steps.

Instead of extrapolating the torque-filling height curve to zero, the results at the lowest filling height (between 0 and 10 mm) were exploited to investigate the influence of the cone. Ideally, the filling height of the vertical part of the inner cylinder was 0 mm, indicating that only the cone was submerged in the concrete, while the vertical wall of the inner cylinder was not. In case the filling height did not exceed 10 mm, the torque was corrected by taking the ratio of the contact surface the cone takes compared to the total contact surface of the cone and the submerged part of the inner cylinder.

For each concrete tested, the rotational velocity was changed in six steps from 0.9 to 0.01 rps. The results of the four steps at the highest rotational velocities, from 0.3 to 0.9 rps were used to determine the influence of the cone, as the results at the lowest rotational velocities have doubtful accuracy due to the low torque registered. For concrete mixtures with plastic viscosity (tested in the ConTec Viscometer 5 (described further)) equal to or higher than 40 Pa s, the torque caused by the cone is considered as a function of the rotational velocity and concrete viscosity. For both parameters, this torque value increased linearly, enabling the fitting of linear equations (Fig. 4). These equations allow the calculation of the effect of the cone for any concrete with plastic viscosity between 40 and 140 Pa s, and for any rotational velocities lower than 0.9 rps. Note that for the lower rotational velocities, the T_{cone} values were extrapolated.

For concrete with plastic viscosity lower than 40 Pa s, the torque is approximated to evolve linearly between zero at (theoretical) zero plastic viscosity and the value obtained at 40 Pa s plastic viscosity.

The correction procedure yields two equations for the torque, Eq. (3) for concrete with plastic viscosity (μ_p) between 40 and 140 Pa s, and Eq. (4) for concrete with plastic viscosity lower than 40 Pa s.

$$T_{cone} = \left(5.38\cdot10^{-4}\mu_p + 1.32\cdot10^{-1}\right)\cdot N + \left(4.28\cdot10^{-4}\mu_p + 4.41\cdot10^{-2}\right) \quad (3)$$

$$T_{cone} = 1.53\cdot10^{-1}\frac{\mu_p}{40}\cdot N + 6.12\cdot10^{-2}\frac{\mu_p}{40} \quad (4)$$

Note that the estimation of the torque caused by the cone of the tribometer is only an approximation, it is not perfect. On the other hand, as the effect is certainly present, it ought to be more useful to perform the correction instead of neglecting the effects. Due to the large vertical part of the inner cylinder, the contribution of the cone to the total torque is in most cases between 5% and 10% for the highest rotational velocity and between 8% and 15% for low rotational velocities.

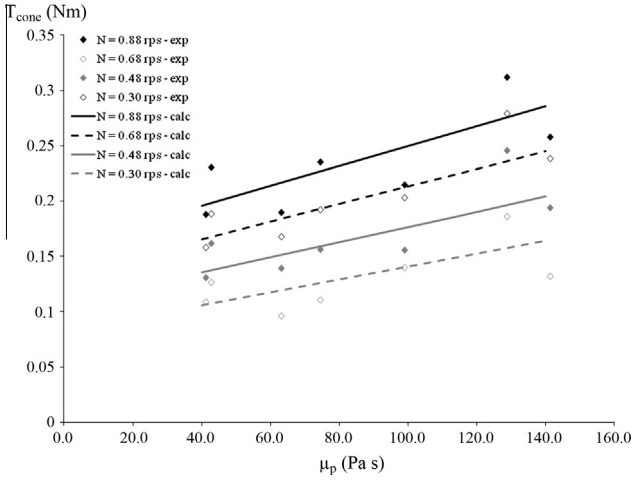

Fig. 4. Linear fitting of the flow resistance caused by the cone for concretes as a function of the plastic viscosity (between 40 and 140 Pa s) and the rotational velocity of the tribometer.

4.4. Data treatment

For each rotational velocity step, the mean values are taken for the torque, provided the data points are in equilibrium. In the next step, the influence of the cone must be subtracted from the torque data, by applying Eq. (3) or Eq. (4). As a result, 10 torque-rotational velocity data points are obtained. The data can then be interpreted in two ways: Either by using the total flow resistance of the concrete in the tribometer as a parameter, or by determining the properties of the lubrication layer.

4.4.1. Total flow resistance in the tribometer

The total flow resistance in the tribometer is reflected by the slope of the torque-rotational velocity curve. This slope is referred to here as I_{trib} and has Nms as unit. As can be seen, the unit of I_{trib} is not a fundamental unit and depends thus on the geometry of the tribometer. Unfortunately, no corresponding fundamental parameter, which is independent of the geometry, can be found for this complex flow, as the sample is no longer homogeneous. On the other hand, as is shown further in this paper, I_{trib} can be a useful parameter when comparing the pumping resistance of different concrete mixtures.

4.4.2. Determination of the lubrication layer properties

4.4.2.1. Theory. When testing concrete inside the tribometer, three different flow conditions can occur, depending on the yield stress of the concrete:

- The lubrication layer is sheared, while the concrete remains unsheared. This is the condition for measuring the tribological properties of CVC, as described in Sections 2 and 3.
- Both the lubrication layer and concrete are entirely sheared.
- The lubrication layer is sheared, and the concrete is partly sheared.

In order to obtain the properties of the lubrication layer, the influence of concrete shearing, if present, must be subtracted. Therefore, it is necessary to perform a rheological measurement on the concrete, separately, to know its intrinsic yield stress and plastic viscosity. If the concrete remains unsheared, which can be evaluated visually, the rheological measurement is not necessary.

The procedure is first explained in case the concrete sample is entirely sheared. This condition can be verified by calculating the plug radius (R_p) with Eq. (5). If R_p is larger than the outer radius (R_o), the entire sample is sheared.

$$R_p = \sqrt{\frac{T}{2\pi\tau_0 h}} \quad (5)$$

At each rotational velocity, the torque, corrected for the bottom effect, is known. As a result, the shear stress evolution between the inner and outer cylinders can be calculated using Eq. (6):

$$\tau(r) = \frac{T}{2\pi h}\frac{1}{r^2} \quad (6)$$

As the Bingham parameters yield stress and plastic viscosity of the concrete are known, the shear rate evolution can be calculated as follows:

$$\dot{\gamma}(r) = \frac{\frac{T}{2\pi h}\frac{1}{r^2} - \tau_0}{\mu_p} \quad (7)$$

Integrating the shear rate over the radius delivers the velocity gradient, and as the velocity at the outer cylinder is zero, the velocity at the boundary between the concrete and the lubrication layer can be calculated. Unfortunately, the thickness of the lubrication layer is unknown. Therefore, as a simplification, the rotational velocity of the concrete is evaluated at the inner cylinder, which is named N_i and can be calculated with Eq. (8). Note that N_i, to be physically 100% correct, denotes the velocity difference between the inner cylinder and the outer cylinder (which is stationary).

$$N_i = \frac{T}{8\pi^2 h \mu_p}\left(\frac{1}{R_i^2} - \frac{1}{R_o^2}\right) - \frac{\tau_0}{2\pi\mu_p}\ln\left(\frac{R_o}{R_i}\right) \quad (8)$$

In fact, the rotational velocity N_i (rps) is the rotational velocity resulting from the shearing of the concrete when imposing a torque T. N_i corresponds to the rotational velocity that would be imposed in a rheometer with exactly the same dimensions to observe a torque T, without the formation of the lubrication layer. As a result, as at each imposed rotational velocity N at the inner cylinder T changes, N_i will be different for each velocity step.

In case the sample is partly sheared ($R_p < R_o$), R_o must be replaced by R_p in Eq. (8). In case the concrete is not sheared, the plug radius will be smaller than the inner radius, and N_i must consequently be equal to zero.

To calculate the properties of the lubrication layer, for each imposed rotational velocity, the corresponding N_i value must be subtracted from the total rotational velocity. As a result, the velocity difference which is overcome by the lubrication layer, referred to here as $N_{LL} = N - N_i$, is obtained. Finally, the yield stress and viscous constant of the lubrication layer are obtained using Eq. (2), as the linear velocity V equals $2\pi R_i N_{LL}$, and the shear stress at the inner cylinder can be calculated according to Eq. (1).

4.4.2.2. Example. The entire procedure is illustrated based on the following example for a HWC with a yield stress of 136 Pa and a plastic viscosity of 94 Pa s, measured in the ConTec Viscometer 5 (described further). In Table 2, the first column indicates the data point number, while columns 2 and 3 contain the corrected torque (with Eq. (3)) and measured rotational velocity (N) data in the tribometer, respectively. In column 4, the plug radius is calculated based on Eq. (5), with as input the yield stress of the concrete and the measured torque at each data point. In this example, the concrete is entirely sheared for the three highest rotational velocities ($R_p > R_o = 118.5$ mm), partly sheared between 0.6 and 0.2 rps and not sheared at all at the two lowest rotational velocities ($R_p < R_i = 65$ mm). Column 6 contains the calculated N_i, according to Eq. (8), in which R_o is used for the three highest rotational velocities, and the corresponding R_p is inserted in the formula for the five next points. If the concrete is not sheared, N_i is logically equal to zero. In columns 7 and 8, N_{LL} and V are calculated, while in column 9, the torque is transformed into a shear stress at the inner cylinder by Eq. (1). Determining the intercept and inclination of the shear stress–linear velocity curves delivers the lubrication layer yield stress ($\tau_{0,LL}$): 1.72 Pa; and viscous constant (η_{LL}): 2311 Pa s/m.

Table 2
Example of the calculation of the lubrication layer properties. Columns 4 and 5 show whether the concrete is fully or partly sheared, or not. Column 6 shows the calculation of the contribution of the concrete shearing to the rotational velocity (N_i) and column 7 shows the velocity difference over the lubrication layer only (N_{LL}).

Pt	T (Nm)	N (rps)	R_p (m)	Concrete sheared?	N_i (rps)	N_{LL} (rps)	V_{LL} (m/s)	τ_i (Pa)
1	2.97	0.87	0.132	Yes	0.22	0.65	0.256	604
2	2.64	0.78	0.124	Yes	0.18	0.59	0.233	539
3	2.40	0.68	0.119	Yes	0.15	0.53	0.207	489
4	2.10	0.58	0.111	Partly	0.12	0.45	0.182	428
5	1.79	0.48	0.102	Partly	0.08	0.40	0.158	365
6	1.45	0.39	0.092	Partly	0.05	0.34	0.133	296
7	1.12	0.29	0.081	Partly	0.02	0.27	0.107	229
8	0.85	0.20	0.070	Partly	0	0.20	0.078	172
9	0.47	0.12	0.052	No	0	0.12	0.046	96
10	0.22	0.01	0.036	No	0	0.01	0.005	46

Note that the value of the viscous constant is rather elevated compared to typical results obtained by Kaplan [6] Chapdelaine [8] and Ngo [23] (around 1000 Pa s/m). This could be due to the low water content, and thus high viscosity of the concrete.

4.4.3. Remarks

The rheological properties of the concrete have been determined with the ConTec Viscometer 5. An attempt has been undertaken to also use the ICAR rheometer, which delivers slightly higher yield stresses but significantly lower plastic viscosities compared to the ConTec [28]. Due to these lower plastic viscosities, the contribution of the concrete shearing to the rotational velocity (N_i) became too large, resulting in negative N_{LL}, which is physically impossible. Therefore, the results of the ConTec are used to estimate the rheological properties of the concrete.

In the next section, a new parameter is introduced as the contribution of the concrete shearing to the total rotational velocity in the tribometer: N_i/N at the rotational velocity closest to 0.5 rps. The higher this factor, the more the concrete shearing contributes to the total flow in the tribometer.

5. Application of the tribometer

5.1. Concretes

In this study, two CVC, four HWC and 23 SCC were produced. These concretes were high-strength, non air-entrained concretes. All concretes were produced with ordinary Portland cement (GU cement), class C fly ash and silica fume, in a 69%–25%–6% mass ratio, or with a 94% OPC–6% silica fume proportion. The reference mixtures for all concrete types had 375 l/m^3 of paste volume and a w/cm = 0.28. The sand-to-total aggregate ratio by mass was kept constant at 0.45, 0.49 and 0.53 for the reference CVC, HWC and SCC respectively. Variations in mix design were the amount of superplasticizer (SP) employed to vary the slump flow, the w/cm (at 0.22, 0.25 and 0.28), the paste volume (350, 375 and 400 l/m^3), the binder composition and the aggregate combination.

For the CVC, HWC and SCC 1–8, natural sand was employed with a fineness modulus of 2.58, a density of 2650 kg/m^3 and an absorption of 1.27%. The 5–14 mm coarse aggregates employed had a density of 2740 kg/m^3 and an absorption of 0.43%. For the other SCC, a combination of four aggregates was used. A very fine dune sand (FM = 0.59, abs = 0.71% and density = 2630 kg/m^3, 97% of particles finer than 300 μm) was combined with a manufactured, coarse sand (FM = 3.53, abs = 2.40% and density = 2700 kg/m^3). The coarse aggregates consisted of crushed limestone, characterized as 0–10 mm (FM = 6.34, abs = 0.68% and density = 2810 kg/m^3) and 10–20 mm (FM = 6.86, abs = 0.63% and density = 2800 kg/m^3). The influence of the aggregates was determined by changing the ratio of fine-to-coarse sand, changing the amount of large and small coarse aggregates and finally by changing the sand-to-total aggregate ratio.

The superplasticizer used is a highly-effective polycarboxylate based high-range water-reducing agent (HRWRA), with an extended workability retention. The amount of SP was adjusted to obtain the desired slump or slump flow, usually around 720–750 mm for SCC. The anticipated compressive strength of the concretes was between 70 and 120 MPa, indicating a relatively high strength. The detailed concrete compositions can be found in Table 3.

Table 3
Mix designs (per m^3) of concretes used for the investigation of the lubrication layer properties.

	GU cement (kg/m^3)	Silica fume (kg/m^3)	Fly ash C (kg/m^3)	Water[a] (kg/m^3)	Natural sand (kg/m^3)	Coarse aggr. 14 mm (kg/m^3)	HRWRA (l/m^3)
CVC 1	372	32	135	151	768	932	1.63
CVC 2	397	35	144	161	739	897	1.67
HWC 1	397	35	144	161	803	830	2.00
HWC 2	369	32	134	150	838	866	2.06
HWC 3	397	35	144	161	803	830	1.91
HWC 4	397	35	144	161	803	830	2.06
SCC 1	397	35	144	161	867	764	2.55
SCC 2	397	35	144	161	867	764	2.74
SCC 3	397	35	144	161	867	764	3.06
SCC 4	397	35	144	161	867	764	3.19
SCC 5	371	32	134	150	902	765	3.15
SCC 6	424	37	154	172	830	731	3.21
SCC 7	541	35		161	902	794	4.64
SCC 8	581	37		173	865	762	4.88

	GU cement (kg/m^3)	Silica fume (kg/m^3)	Fly ash class C (kg/m^3)	Water[a] (kg/m^3)	Fine sand (kg/m^3)	Crushed sand (kg/m^3)	C aggr. 10 mm (kg/m^3)	C aggr. 20 mm (kg/m^3)	HRWRA (l/m^3)
SCC 21	397	35	144	161	224	721	328	354	3.45
SCC 22	397	35	144	161	160	786	328	354	3.73
SCC 23	397	35	144	161	96	850	328	354	4.00
SCC 26	397	35	144	161	224	722	434	245	3.36
SCC 27	397	35	144	161	224	722	533	143	3.59
SCC 28	397	35	144	161	213	685	572	153	3.36
SCC 29	397	35	144	161	202	648	611	164	3.45
SCC 30	397	35	144	161	224	722	533	143	3.36
SCC 31	397	35	144	161	224	722	533	143	3.59
SCC 32	418	36	151	152	224	720	531	143	4.86
SCC 33	439	38	159	141	224	719	531	143	7.27
SCC 34	581	37		173	224	720	531	143	4.59
SCC 35	611	39		163	224	719	531	143	6.55
SCC 36	645	41		153	223	719	530	143	10.91

[a] Including the SP water content.

5.2. Mixing and testing procedure

After the determination of the humidity of the sand, all aggregates were added to the drum mixer with half of the mixing water. After 2 min of mixing to ensure homogeneity, all cementitious materials were added and mixed for 30 s, followed by the superplasticizer which was diluted in the second half of the mixing water. Mixing continued for 3 min after which the homogeneity of the mixture was verified and if necessary, the walls of the mixer were manually scraped. Mixing continued for 2.5 more minutes, followed by a rest of 1 min. Before evaluating the slump flow, mixing resumed for 2 additional minutes. If an extra addition of SP was necessary, the mixing resumed for 1 min. Note that this mixing procedure is quite extensive, but this is necessary due to the low water content and the high viscosity of the mixtures.

After mixing, the slump flow and V-funnel flow time were measured 15 min after the contact between cement and water. At 30 min of age, concrete samples were placed simultaneously in the ConTec Viscometer 5 and in the tribometer to evaluate the rheological and tribological properties. The workability and rheology/tribology tests were repeated 3 more times, each time with a 30 min interval. In order to exclude uncertainties induced by small errors in rheological and tribological measurements, the four rheological and tribological measurements were averaged and are represented by a single value in this paper. As the employed admixture showed high workability retention, the rheological and tribological values remained approximately constant with time.

Fig. 5. ConTec Viscometer 5 used for the measurement of the rheological properties of concrete.

5.3. ConTec Viscometer 5

The rheological properties of the concretes were evaluated using the ConTec Viscometer 5 (Fig. 5). This rheometer, suitable for concretes with a maximum aggregate size of 16 mm, is based on the principle of the coaxial cylinders. The outer cylinder, with a radius of 145 mm rotates at a predefined set of rotational velocities, while the resulting torque is measured at the inner cylinder, which has a radius of 100 mm. The inner cylinder consists of two parts: the torque is only measured at the upper part of the inner cylinder, while the lower part eliminates the complex 3-D flow effects from the measuring zone [18]. The height of the upper part of the inner cylinder submerged in the concrete is measured after each test, and averages 110 mm. Both cylinders are equipped with protruding ribs in order to avoid, or at least minimize, the horizontal movement of aggregates and thus the creation of a lubrication layer.

During a rheometer test, the concrete is subjected to a stepwise decrease in rotational velocity from 0.5 to 0.025 rps in 10 steps. Each step takes 5 s. The testing is preceded by a 20 s pre-shearing period at the maximum rotational velocity to eliminate as much as possible the effect of thixotropy. After taking the average of the torque and rotational velocity for each data point, the Reiner–Riwlin equation was applied to obtain the yield stress and plastic

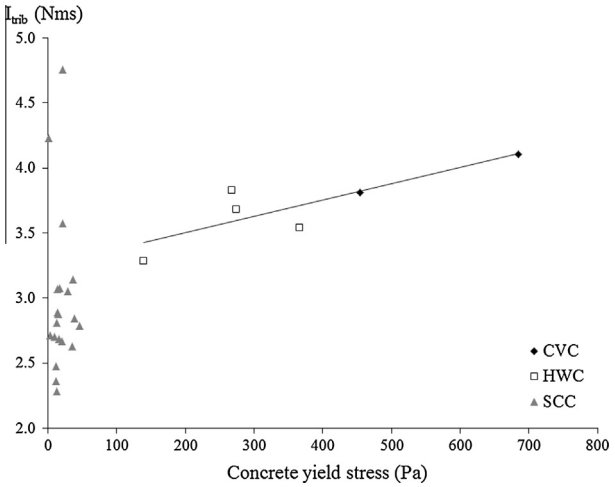

Fig. 6. The total flow resistance in the tribometer (I_{trib}) is well related to the concrete yield stress for CVC and HWC. For SCC, I_{trib} is lower than for CVC and HWC, but no clear relation with the yield stress is observed.

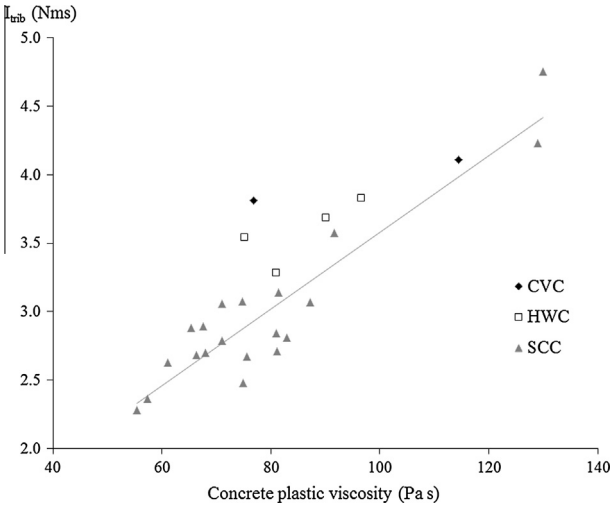

Fig. 7. The total flow resistance in the tribometer (I_{trib}) is well related to the concrete plastic viscosity for SCC.

Table 4
Average of four tests of rheological and tribological properties for all concretes. The residuals of the viscous constant are the differences between then measured viscous constant the predicted viscous constant by means of concrete viscosity and Fig. 8. The contribution of the concrete shearing to the flow in the tribometer at 0.5 rps indicates how essential the formation of the lubrication layer is.

	Initial SF * = slump (mm)	Yield stress (Pa)	Plastic visco (Pa s)	I_{trib} (Nms)	Viscous constant (Pa s/m)	Contrib. concrete shearing (%)	Residual viscous constant (Pa s/m)	Difference with ref.
CVC 1	185*	684	115	4.11	2131	0.0		PV = 350
CVC 2	220*	455	77	3.81	2044	0.1		REF CVC
HWC 1	500	274	90	3.68	2210	4.0		REF HWC
HWC 2	500	268	97	3.83	2443	8.6		PV = 350
HWC 3	445	366	75	3.54	1993	0.9		SF = 450
HWC 4	545	139	81	3.29	2553	20.9		SF = 550
SCC 1	620	46	71	2.79	2293	27.4	−310	SF = 620
SCC 2	670	39	81	2.84	2420	34.5	−323	SF = 670
SCC 3	720	16	66	2.69	2723	46.8	188	REF SCC 1
SCC 4	765	3	81	2.71	2390	41.6	−356	SF = 760
SCC 5	725	36	81	3.14	2808	34.4	59	PV = 350
SCC 6	720	14	68	2.89	3119	51.8	565	PV = 400
SCC 7	700	21	92	3.58	3359	38.5	465	PV = 350, no FA
SCC 8	710	28	71	3.06	3219	45.1	618	PV = 375, no FA
SCC 21	720	14	87	3.07	2687	34.5	−145	Change in aggregate
SCC 22	710	13	83	2.81	2414	35.3	−356	grading curve SCC 27 = REF SCC 2
SCC 23	725	11	75	2.48	2130	36.9	−527	
SCC 26	730	21	76	2.67	2385	38.1	−282	
SCC 27	745	9	68	2.70	2647	45.4	88	
SCC 28	715	15	65	2.88	3147	46.8	624	
SCC 29	720	17	75	3.08	3155	44.0	499	
SCC 30	720	13	55	2.28	2311	47.1	−70	
SCC 31	725	12	57	2.37	2413	47.5	5	
SCC 32	750	0	129	4.23	3763	37.7	341	w/cm = 0.25
SCC 34	710	35	61	2.63	2581	37.4	119	w/cm = 0.28, no FA
SCC 35	715	22	130	4.75	4422	42.8	987	w/cm = 0.25, no FA
SCC 33	765		250	7.49	6535	33.4		w/cm = 0.22
SCC 36	710		342	7.77	5380	26.1		w/cm = 0.22, no FA

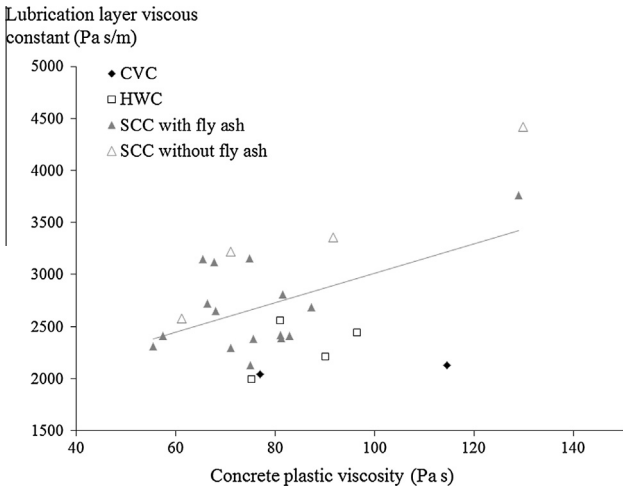

Fig. 8. The viscous constant shows a relationship with the concrete plastic viscosity for SCC. The hollow triangles represent the SCC mixtures without fly ash, showing higher viscous constants than the mixtures with fly ash. CVC and HWC show generally lower viscous constants compared to SCC. The drawn relationship between the viscous constant and concrete viscosity is based on the SCC mixtures with fly ash. This relationship is used for the analysis of the residuals.

viscosity from the (T,N) data. Potential measurement artefacts, such as thixotropy, segregation, and plug flow, were investigated carefully. If necessary, data points were corrected or removed from the results, or the measurement was deemed invalid.

5.4. Interpretation of tribological properties

5.4.1. Total flow resistance in tribometer compared to concrete rheological properties

Figs. 6 and 7 show the relationship between the total flow resistance in the tribometer and the concrete yield stress and plastic viscosity, respectively. All rheological and tribological properties, as well as the initial slump flows of all mixtures are shown in Table 4. A good relationship between I_{trib} and the concrete yield stress is obtained for the CVC and the HWC. This relationship can be further extended to the SCC range, but for yield stresses lower than 100 Pa, the correlation between yield stress and I_{trib} is not clear anymore. For SCC however, a clear correlation between I_{trib} and the concrete viscosity is obtained, but for the HWC and the CVC, the correlation is not as clear. This is in accordance with the observed relationships in the literature. For CVC, it is known through the practical guidelines that increasing slump (and thus reducing yield stress) reduces pumping pressure [11–14]. This relationship can be attributed to the capacity of the concrete to form the lubrication layer. On the other hand, it has been recently observed that for SCC, the plastic viscosity is the more dominant factor for the pumping pressure [27,29]. This is the result of the shearing of the concrete in the pipes. As the total flow resistance in the tribometer, I_{trib}, follows both statements, it appears that I_{trib} can be a useful parameter for a preliminary evaluation of the pumping pressure.

Table 5
Sieve stability values of SCC mixtures with and without fly ash for different paste volume, w/cm and aggregate combinations. The results show that the tested SCC mixtures without fly ash have a larger static stability.

	With FA	Sieve stab (%)	Without FA	Sieve stab (%)
PV = 350	SCC 5	6.2	SCC 7	4.6
PV = 375	SCC 3	8.8	SCC 8	5.7
w/cm = 0.28	SCC 27	8.9	SCC 34	5.7
w/cm = 0.25	SCC 32	10.8	SCC 35	7.8

5.4.2. Viscous constant and contribution of concrete to flow

Fig. 8 shows for the SCC mixtures a relatively good correlation between the viscous constant of the lubrication layer and the concrete plastic viscosity. The yield stress of the lubrication layer is not considered in this analysis, as it was negligible for all SCC. The relationship obtained in Fig. 8 is similar to the conclusions of Kaplan [6] and Chapdelaine [8]. Kaplan stated that a relationship between the viscous constant and the concrete viscosity must exist, based on the application of the Farris model and dependent on the possible thickness of the lubrication layer [6]. Chapdelaine concluded that this relationship is valid as long as not too many parameters are varied at the same time [8].

As can be noticed from Fig. 8, the viscous constant of SCC is generally higher than the viscous constant of CVC and HWC. Due to the lower yield stress of SCC, the material chooses the most efficient way to flow, finding a compromise between shearing the bulk concrete and segregation to form the lubrication layer. It appears thus that for SCC, the lubrication layer is less necessary to flow, especially as the total flow resistance in the tribometer (I_{trib}) is mostly lower for SCC.

5.4.2.1. Physical phenomena involved in the formation of the lubrication layer. The lubrication layer is formed by dynamic segregation of (coarse) aggregates away from the zone with the highest shear rate. This zone is the pipe wall during pumping and the inner cylinder of the tribometer. This dynamic segregation phenomenon is stopped, theoretically, when the aggregates in the bulk concrete reach maximum packing. In case the bulk concrete is sheared, dilatancy prevents the maximum packing of the coarse aggregates, pushing them back toward the inner cylinder when they need to pass each other. In CVC, there is no shearing, so the aggregates can reach maximum packing in the bulk concrete. In SCC however, the concrete tries to find the equilibrium between the formation of the lubrication layer and the increase in bulk rheological properties of the concrete due to the increase in particle concentration.

In the following sections, the influence of different mix design parameters on the viscous constant and the formation of the lubrication layer are discussed. Apart from the bulk rheological properties, the total flow resistance in the tribometer (I_{trib}) and the viscous constant, two other parameters are used in the discussion. The first parameter is the contribution of the concrete shearing to the total flow in the tribometer at 0.5 rps. This parameter indicates the necessity of the concrete to form the lubrication layer. The second parameter is called the residual of the viscous constant

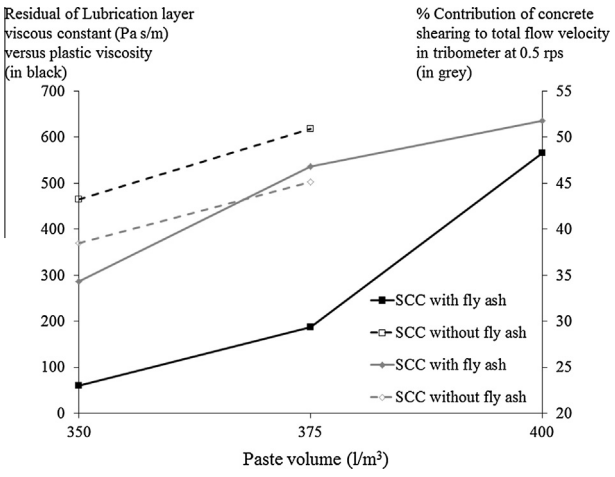

Fig. 9. Both the residual in viscous constant (black) and the concrete shearing contribution (gray) increase with increasing paste volume, indicating that the lubrication layer is less necessary at higher paste volumes.

compared to the concrete viscosity. In Fig. 8, for all SCC mixtures with fly ash, the relationship between the viscous constant and concrete viscosity is determined. The residuals of the viscous constant are thus the difference between the experimental value and the value the viscous constant should have at the specific plastic viscosity. A positive residual indicates a larger viscous constant, while a negative value is a smaller viscous constant compared to the reference line. With these two parameters, the influence of the mix design on the lubrication layer can be further explored.

5.4.2.2. Influence of binder composition. In Fig. 8, the SCC mixtures are displayed in two groups, depending on the binder composition. The mixtures without fly ash showed a higher viscous constant at a certain viscosity, compared to the mixtures with fly ash. This is also clear in Table 4 and similar results are obtained for I_{trib}. The trendline displayed in Fig. 8 is therefore only based on the SCC mixtures with fly ash, excluding the mixture with w/cm = 0.22 due to doubts on the accuracy of the mixture and the rheological measurements. It appears thus that the viscous constant of mixtures without fly ash is higher, which can be attributed to a higher viscosity or smaller thickness of the lubrication layer. Table 5 shows the static segregation results measured with the sieve stability test [30] for SCC 3, 5, 7, 8, 27, 32, 34 and 35. Comparing the mixtures with and without fly ash for equal paste volume, w/cm and aggregate combination delivers systematically a greater static stability for the SCC mixtures without fly ash. As a consequence, it can be expected that the mixtures without fly ash also show a larger resistance to dynamic segregation, which is the driving phenomenon for the formation of the lubrication layer.

5.4.2.3. Influence of paste volume. The paste volume is expected to be a critical factor in the formation and properties of the lubrication layer, as it determines how much cement paste can migrate to the lubrication layer. The plastic viscosity, total flow resistance in the tribometer (I_{trib}) and the lubrication layer viscous constant all decrease with an increase in paste volume from 350 to 375 l/m^3. Increasing the paste volume to 400 l/m^3 did however not induce a large variation in concrete viscosity and I_{trib}, and caused even an increase in the viscous constant (see Table 4). Fig. 9 shows the results of SCC 3 and SCC 5–8. The distinction is made between mixtures with and without fly ash. The residuals of the viscous constant show a steady trend with an increase in paste volume: the larger the paste volume, the more the viscous constant increases, compared to the relationship with the plastic viscosity. The specific reason for this phenomenon is still unknown, but it

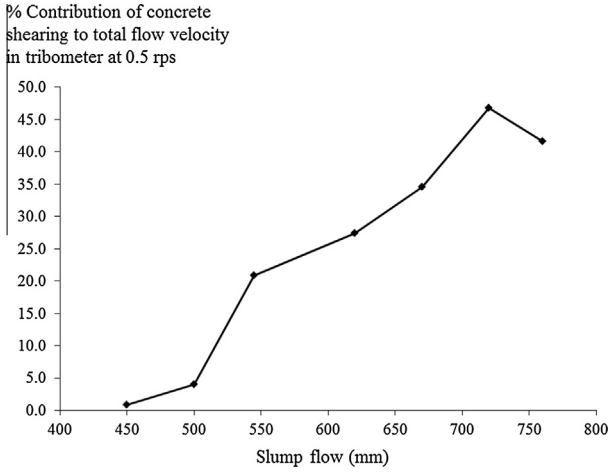

Fig. 10. The contribution of the concrete shearing logically increases with increasing slump flow, as lower stresses are needed to make the concrete flow.

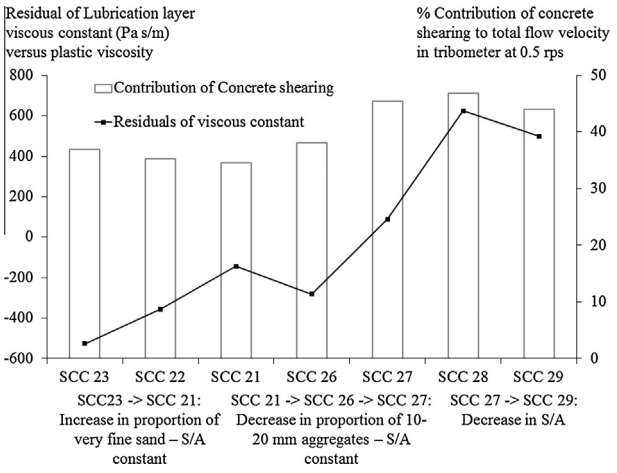

Fig. 11. Influence of the grain size distribution (% fine sand to total sand, % 20 mm aggregates to total coarse aggregates and S/A) on the residuals of the viscous constant and the contribution to concrete shearing.

is expected that the easier flow of concrete with high paste volumes has an effect. Indeed, as shown in Fig. 9, the contribution of concrete shearing to the total flow velocity in the tribometer (at 0.5 rps) increases with increasing paste volume, rendering the formation and properties of the lubrication layer less important compared to concretes with lower paste volumes.

5.4.2.4. Influence of w/cm. The w/cm of the high-strength SCC mixtures was decreased from 0.28 (reference value) to 0.25 and 0.22 (respectively SCC 27, 32 and 33 with fly ash and SCC 34, 35 and 36 without fly ash). The concrete viscosity, I_{trib}, and viscous constant largely increase with a decrease in w/cm (Table 4). However, the measurements on the w/cm = 0.22 mixture can be doubted, as difficulties arose to have a well dispersed SCC with the described mixing procedure. The analysis on the residuals of the viscous constant (compared to concrete viscosity) is deemed inaccurate as the relationship between viscous constant and concrete viscosity is determined for concrete viscosities between 40 and 100 Pa s. However, the contribution of the concrete shearing to the total flow in the tribometer decreases with decreasing w/cm, indicating an increasing importance of the lubrication layer. As the concrete is significantly more viscous, despite the reduction in dynamic segregation [31], the concrete shows a larger tendency to form the lubrication layer.

5.4.2.5. Influence of yield stress. Comparing SCC mixtures 1–4 determines the influence of the initial slump flow (or yield stress) on the viscous constant. The concrete viscosity, I_{trib} and the viscous constant appear more or less unaffected by the initial slump flow (Table 4). The contribution of the concrete shearing to the total flow in the tribometer increases with increasing slump flow (Fig. 10). This result is quite logical as a decrease in yield stress causes a larger shear rate at equal shear stress. Considering HWC 1, 3 and 4, which had a similar mix design compared to SCC 1–4, except for a lower S/A and a lower initial slump flow, the same conclusions can be drawn. Although, the viscous constant appears to decrease with decreasing initial slump flow, which may be the consequence of the larger importance of the lubrication layer on the flow in the tribometer.

5.4.2.6. Influence of aggregate combination. SCC mixtures SCC 21–23 and 26–29 all had a different aggregate grain size distribution, while all other parameters remained constant. For SCC 21–23, the proportion of very fine sand was decreased, while the S/A

remained constant. For SCC 21, 26 and 27, the amount of coarse aggregates 10–20 mm was decreased, keeping the S/A constant. SCC 27–29 were produced to verify a decrease in S/A, while keeping the combinations of sand and coarse aggregates constant.

Decreasing the amount of very fine sand decreased the concrete viscosity, I_{trib} and the viscous constant. It also reduced more importantly the viscous constant than the concrete viscosity, as the residuals are negative (Fig. 11). As the very fine sand particles have a large specific surface area, more cement paste is needed to coat these particles, increasing the viscosity of the mortar and the concrete. On the other hand, somewhat surprisingly, the contribution of the concrete shearing to the flow in the tribometer increased slightly with decreasing very fine sand amount. It is thus more favorable for the concrete to shear instead of forming the lubrication layer, despite the lower viscous constant.

Replacing partially the 10–20 mm coarse aggregates by 0–10 mm coarse aggregates reduced significantly the concrete viscosity, affected slightly I_{trib}, and showed an apparent optimal value for the viscous constant. The analysis of the residuals on the viscous constant are related to the large increase in viscous constant between SCC 26 and SCC 27, while the contribution of the concrete shearing increased when reducing the 10–20 mm aggregate portion in the concrete (Fig. 11). Potential explanations could be found in the theories of dynamic segregation, packing density and dilatancy, but no specific reason has been found for this phenomenon.

A decrease in S/A slightly increased the concrete viscosity, I_{trib}, but a larger increase in the viscous constant was noted. The contribution of the concrete shearing to the total flow in the tribometer remained relatively constant however (Fig. 11).

5.4.2.7. Summary. There exists a relationship between the viscous constant of the lubrication layer and the plastic viscosity of the concrete, but a significant number of parameters affect this relationship. The binder composition, paste volume, w/cm, concrete yield stress and aggregate grading curves show an influence on the ratio of viscous constant to plastic viscosity. As stated by Chapdelaine, the relationship between viscous constant of the lubrication layer and the concrete viscosity becomes rather complicated if a lot of parameters are involved. The results discussed above confirm this statement, as a detailed analysis on the phenomena involved appears not straightforward. It is expected that dynamic segregation, particle packing and dilatancy have an effect on the formation, viscosity and thickness of the lubrication layer. The effect of dynamic segregation is insinuated by the influence of the binder composition, w/cm and grain size distribution. Particle packing influences the potential maximum thickness of the lubrication layer, but it is expected that due to the shearing of the concrete and the dilatancy of the coarse aggregates, this maximum thickness cannot be achieved. Note that for non-sheared concrete, such as CVC, the maximum thickness can theoretically be obtained in the tribometer. Highly workable concretes show a complex equilibrium between shearing of the bulk concrete and the formation of the lubrication layer inside the tribometer. It is expected that a similar equilibrium is obtained during pumping of this type of concrete.

6. Conclusions

Concrete tribometers have been used in the past to characterize the properties of the lubrication layer which is formed near the pipe wall during pumping of concrete. The lubrication layer properties are expressed as a yield stress (in Pa) and a viscous constant (in Pa s/m), which incorporates the lubrication layer viscosity and thickness. In order to measure the lubrication layer properties, the concrete itself was not allowed to be sheared, restricting the application of these apparatuses for highly-workable concretes, including self-consolidating concrete. Based on the restrictions of the previously developed tribometers, a new design for a tribometer is proposed. It consists of a large, smooth steel cylinder rotating in a concrete bucket. The bottom of the inner cylinder is cone-shaped, facilitating the insertion of the cylinder in the concrete.

A procedure is proposed to correct the 3-D influence of the cone as a function of the rotational velocity and the concrete plastic viscosity. Although the influence of the cone is rather small compared to the total torque measured, it seems better to subtract this influence from the total torque value at each rotational velocity.

The properties of the lubrication layer can be determined if the contribution of concrete shearing to the rotational velocity is known. Therefore, it is necessary to perform a rheological measurement on concrete to retrieve its rheological properties in parallel with the tribological test. Based on the rheological properties of the concrete, a calculation procedure is shown, taking into account whether the concrete is fully, partly or not sheared. Note that the choice of the rheometer can influence the results obtained with the tribometer.

Based on the described procedure, the properties of the lubrication layer for several concretes have been calculated. The total flow resistance of the tribometer, called I_{trib}, relates well to the concrete yield stress for CVC and HWC, which is in accordance to the practical guidelines for pumping of concrete. For SCC however, I_{trib} relates better to the plastic viscosity of the concrete, which is in agreement with recent literature on pumping of SCC.

There exists a relationship between the viscous constant of the lubrication layer and the plastic viscosity of the concrete, but a significant number of parameters influence this relationship. Highly workable concretes (including SCC) tend to find a complex equilibrium between shearing the bulk concrete and forming the lubrication layer. Mix design parameters such as the binder composition, paste volume, w/cm, initial slump flow and aggregate grain size distribution have been investigated to find this equilibrium. Omitting the fly ash reduced dynamic segregation potential, leading to a higher viscous constant compared to the mixtures with fly ash. Increasing paste volume reduced the necessity for forming the lubrication layer, and a similar result was obtained for a decrease in yield stress. Decreasing the w/cm to 0.25 and 0.22 increased the importance of the lubrication layer. However, the formation of lubrication layer is complex as it involves dynamic segregation, particle packing and dilatancy. On the other hand, it has been shown that this tribometer is a useful tool for the study of the lubrication layer formation and properties.

Acknowledgements

The authors would like to acknowledge Sodamco for the financial support of the research project and the technical staff of the Université de Sherbrooke for the construction of the tribometer and the help with the execution of the experiments.

References

[1] Ede AN. The resistance of concrete pumped through pipelines. Mag Concr Res 1957;9:129–40.
[2] Morinaga M. Pumpability of concrete and pumping pressure in pipeline. In: Proc RILEM seminar on fresh concrete: important properties and their measurement, Leeds, vol. 7; 1973. p. 1–39.
[3] Browne RD, Bamforth PB. Tests to establish concrete pumpability. ACI J 1977;74:193–203.
[4] Chalimo T, Touloupov N, Markovskiy M. Peculiarities of concrete pumping, Minsk; 1989 [in Russian].
[5] Sakuta M, Kasanu I, Yamane S, Sakamoto A. Pumpability of fresh concrete. Tokyo: Takenaka Technical Research Laboratory; 1989.
[6] Kaplan D. Pompage des bétons. Ph-D dissertation. Paris: Laboratoire Central des Ponts et Chaussées; 2001 [in French].
[7] Jolin M, Chapdelaine F, Gagnon F, Beaupré D. Pumping concrete: a fundamental and practical approach. In: Proc of the 10th conf on shotcrete for underground support, Whistler; 2006.

[8] Chapdelaine F. Etude Fondamentale et Pratique sur le Pompage du Béton. Ph-D dissertation. Laval: Université Laval; 2007 [in French].
[9] Jodeh SA, Nassar GE. Pumpability assessment of C90 SCC. In: Proc of the 2nd int conf on advances in concrete technology in the Middle-East: self-consolidating concrete, Abu Dhabi; 2009. p. 155–76.
[10] Aldred J. Burj Khalifa – a new high for high-performance concrete. Proc of the ICE – Civil Eng 2010;163(2):66–73.
[11] Eckardstein Karl Ernst V. Pumping concrete and concrete pumps – a concrete placing manual. Schwing; 1983. 133 p.
[12] Crepas RA. Pumping concrete, techniques and applications. 3rd ed. Elmhurst: Crepas and Associates Inc.; 1997.
[13] ACI-Committee 304. Placing concrete by pumping methods. Farmington Hills: American Concrete Institute; 1998.
[14] ASTM C 33. Standard specification for concrete aggregates. Philadelphia: American Society for Testing and Materials; 2003.
[15] Kaplan D, Sedran T, de Larrard F, Vachon M, Marchese G. Forecasting pumping parameters. In: Proc of the 2nd int rilem symp on self compacting concrete, Tokyo; 2001. p. 555–64.
[16] Tattersall GH, Banfill PFG. The rheology of fresh concrete. London: Pitman; 1983.
[17] Wallevik OH. Rheology – a scientific approach to develop self-compacting concrete. In: Proc of the 3rd int symp on self-compacting concrete, Reykjavik; 2003. p. 23–31.
[18] Wallevik OH. Introduction to rheology of fresh concrete, course compendium. Reykjavik: ICI Rheocenter Course – Reykjavik University; 2009.
[19] Reiner M. Deformation and flow; an elementary introduction to theoretical rheology. Great Britain: H.K. Lewis & Co. Limited; 1949.
[20] Wallevik JE. Rheology of particle suspensions – fresh concrete, mortar and cement paste with various types of lignosulfonates. Ph-D dissertation. Department of Structural Engineering, The Norwegian University of Science and Technology, Trondheim. <www.diva-portal.org>; 2003.
[21] Macosko CW. Rheology principle, measurements and applications. New-York: Wiley-VCH; 1994.
[22] De Larrard F, Hu C, Sedran T, Szitkar JC, Joly M, Claux F, et al. A new rheometer for soft to fluid fresh concrete. ACI Mater J 1997;94(3):234–43.
[23] Ngo TT. Influence of concrete composition on pumping parameters and validation of a prediction model for the viscous constant. Ph-D dissertation. Université Cergy-Pontoise; 2009 [in French].
[24] Wallevik JE. Rheological properties of cement paste: thixotropic behavior and structural breakdown. Cem Concr Res 2009;39(1):14–29.
[25] Jacobsen S, Haugan L, Hammer TA, Kalogiannidis E. Flow conditions of fresh mortar and concrete in different pipes. Cem Concr Res 2009;39(11):997–1006.
[26] Feys D, Verhoeven R, De Schutter G. Extension of the Poiseuille formula for shear-thickening materials and application to self-compacting concrete. Appl Rheol 2008;18(6):62705.
[27] Feys D. Interactions between rheological properties and pumping of self-compacting concrete. Ph-D dissertation. Ghent, Universiteit Gent; 2009.
[28] Feys D, Khayat KH. Comparing rheological properties of SCC obtained with the ConTec and ICAR rheometers. In: Proc of the 5th North-American conference on self-consolidating concrete, Chicago; 2013.
[29] Feys D, De Schutter G, Verhoeven R. Parameters influencing pressure during pumping of self-compacting concrete. Mater Struct 2013;46:533–55.
[30] EFNARC European Project. The European guidelines for self-compacting concrete: specification, production and use. EFNARC; 2005.
[31] Esmaeilkhanian B, Feys D, Khayat KH, Yahia A. New test method to evaluate dynamic stability of self-consolidating concrete. ACI Mater J 2014;111(1–6) [January–December, MS No. 2012-258, available online].